Surface stress in d-band metal surfaces

2010 J. Phys.: Condens. Matter 22 135007

(http://iopscience.iop.org/0953-8984/22/13/135007)

J. Phys.: Condens. Matter **22** (2010) 135007 (8pp) doi:10.1088/0953-8984/22/13/135007

Surface stress in d-band metal surfaces

M Blanco-Rey and S J Jenkins

Department of Chemistry, University of Cambridge, Lensfield Road, Cambridge CB2 1EW, UK

E-mail: mb633@cam.ac.uk

Received 18 November 2009, in final form 22 January 2010
Published 12 March 2010
Online at stacks.iop.org/JPhysCM/22/135007

Abstract

Using calculations within the density functional approach, we make a survey of the surface stresses of relevant d-band metal surfaces. Unlike the case for surface energies, where volcano-shaped dependences have been found across the d period, the surface stress values show a non-trivial dependence on the metal species and surface termination, which cannot be anticipated from homogeneous electron gas models. A qualitative interpretation as regards the origin of this dependence can be given on the basis of the decomposition of the surface stress into repulsive and attractive electronic components.

(Some figures in this article are in colour only in the electronic version)

1. Introduction

Surface creation upon crystal cleavage produces a free energy increase. This thermodynamic quantity, per unit of created surface at constant temperature, is the so-called surface energy, γ. The atoms in the surface region relax from their bulk-terminated positions and the surface can eventually reconstruct. Such processes occur in order to lower γ. However, despite the system as a whole being in equilibrium, the bulk imposes its equilibrium lateral periodicity on the surface geometry; γ has to be minimized under this constraint and surface atoms are therefore under stress. Formally, this spontaneous surface stress, $[\sigma_{ij}]$, is quantified as the in-plane strain derivative of γ (Shuttleworth equation) [1]. Therefore, $[\sigma_{ij}]$ contains non-local information about γ as a function of the equilibrium crystal in-plane lattice vectors. In recent literature an active debate on the surface stress definition is found [2–11], which can be cleared out for our purposes by a suitable reference coordinates convention when calculating the strain derivative [12].

The role of surface stress in reconstruction has also been a matter of controversy [13–16]. The minimum γ principle, always subject to bulk lateral periodicity constraints, dictates the existence of reconstructed phases. Extensions to this argument, invoking minimization of stress, cannot be made in cases where the reconstruction is dramatic, e.g. when a large amount of mass transport is involved. Since $[\sigma_{ij}]$ is a derivative of γ, it provides the directions towards smaller γ values that are valid only in a small region of the surface configuration space. Therefore, it would be precipitate to say that a stress reduction is the driving force for such reconstructions. In fact, in the case of Ir{110}-(1 × 2) the surface stress does not decrease [17], contradicting that idea. On the other hand, a large stress reduction is observed in cases such as the (1 × 4) reconstruction of anatase TiO_2(001) [18], so it must be acknowledged that, if not a driving force, an underlying correlation between stress relief and reconstruction exists in some systems. Phenomenological correlations have been established also for the general case of the (1 × 2) reconstruction in Au, Ir and Pt {110} surfaces [19, 20].

Surface stress has its origin in the charge distribution at the surface region bonds, which differs from that of bulk because of the lower coordination of surface atoms, and is also linked to atomic relaxations. It is not experimentally accessible from currently available techniques, and only indirect measures can be made on it, e.g. changes in $[\sigma_{ij}]$ upon adsorption or between facets in a surface [21, 12, 22]. Density functional theory (DFT) methods are widely used for stress calculations under suitable convergence conditions, usually following the stress theorem introduced by Nielsen and Martin [23–30] that can be exploited to be used as a complement of experiments. An alternative way of calculating the surface stress consists in removing a transversal section of the surface keeping the remaining atoms and electron density in place. The stress is the Coulomb electrostatic force acting on the remaining atoms per unit length along the cut direction [22].

Based on simple charge redistribution arguments, it can be postulated that electropositive adsorbates, like hydrogen, would produce a tensile change in the stress (i.e. positive), which favours in-plane contraction of atoms, as those donated electrons populate surface bonds, contracting them. On the other hand, electronegative atoms, like oxygen, would

produce a compressive stress (i.e. favours expansion of surface bonds), as the surface atoms donate electrons to fill in the adatom orbitals [22]. However, DFT calculations on Pt{111} yield a compressive stress change upon adsorption of both H and O, which seems to contradict the charge rearrangement picture [31]. The tensile stress relief is alternatively explained by the fact that surface Pt atoms neighbouring adsorption sites gain coordination and Pt valence electrons can distribute isotropically in both cases, along with an expansion of the outermost interlayer Pt–Pt distance [31]. Another representative case is the stress induced in Mo{110} by Li adsorption, which shifts from tensile to compressive with increasing Li coverage. At low coverage, electrons are donated into low lying Mo bonding states and at high coverages, antibonding states begin to fill in [32]. It is worth noticing that the charge redistribution argument is based in the Coulomb force approach, so if these forces were to be calculated accurately for these systems, the apparent contradiction would probably disappear. However, in most DFT codes this task is more complex than stress evaluation through the stress theorem. These examples make it clear that the relationship between $[\sigma_{ij}]$ and surface bond population has non-trivial character. Thus its value cannot be anticipated in general, neither using charge redistribution arguments, nor from geometry relaxation trends.

It is not possible to establish definitively the accuracy of the theoretical methodologies for intrinsic stresses, and for adsorbate induced surface stresses in metallic surfaces the agreement between theory and experiment is highly dependent on the systems under study [33]. For instance, excellent agreement of the order of $\sim$0.02 eV Å^{-2} is found in the surface alloy Mn/Cu{100}-c(2 × 2) [34, 35] and $\sim$0.06 eV Å^{-2} is found in C/Ni{100}-c(2 × 2) [36, 22]. However, large discrepancies of $\sim$0.1 eV Å^{-2} exist in other systems such as oxygen adsorption on Cu{100} [37], Ni{100} [38, 36, 39] or W{110} [40, 39], despite the geometry optimized structures within DFT being, in general, in good agreement with the corresponding experimental ones.

In bulk materials, stress amounts to zero as the kinetic repulsion (yielding a compressive stress contribution) between electrons is compensated by electrostatic attraction and a small tensile stress contributed by exchange and correlation[1]. These components can be isolated within typical DFT calculations [29, 30]. In the presence of a surface, though, those two terms do not balance. For metals, tensile surface stresses are found. Al and Pb are nearly free-electron-like metals, and a jellium model [41] can explain, even semi-quantitatively, some surface stress features [42–44]. In Au, attractive sp bonding counteracts d–d closed shell repulsive interaction, and bond order enhancement at the surface has been invoked to explain tensile stress in Au{100} [45]. These models are not applicable for d-band metals though, where anisotropic effects are expected to be complex due to strong directionality in bonds and varying orbital overlap.

In the present paper, we show a DFT analysis of the surface stress of a number of d-metal surfaces, both in isotropic and anisotropic cases, paying special attention to surfaces sharing structural similarities, to gain insight into the behaviour of magnitude and anisotropy of $[\sigma_{ij}]$. In previous calculations on d-band bcc metals, we found that, for a given metal species, a phenomenological connection exists between surface terminations, such that $[\sigma_{ij}]$ of a low symmetry surface can be roughly anticipated from the value of $[\sigma_{ij}]$ at higher symmetry surfaces with common structural features, namely an in-plane close-packed chain of atoms [46].

It has been observed that γ has a 'volcano-shaped' variation across the d period [47, 48] (with some exceptions for 3d metals [49]), which can be qualitatively accounted for by a simple square-shaped d-band model. In the present paper, we make a survey of d-band metal surfaces, covering representative species and both isotropic and anisotropic surfaces. We do not find such a systematic dependence on the crystal structure or the atomic species and d-band filling for $[\sigma_{ij}]$. This result confirms that the origin of this fundamental property relies upon fine details of the surface electronic structure.

The paper is organized as follows: in section 2 the methodology is described, together with the description of terms contributing to stress; section 3 shows the surface geometries and associated stresses; in section 4 the obtained results are discussed in the context of the existing models in the literature and are correlated with charge redistribution effects at the surface.

2. Calculations

First principles calculations were carried out in the same fashion as those of [46], with the computer code CASTEP [50] and using finite slabs and the supercell approach to approximate surfaces. This code expands wavefunctions using a plane wave basis set and describes ion cores in the pseudopotential approach [50]. In this work, the gradient corrected exchange and correlation functional approach in the Perdew–Wang formulation (PW91) [51] and ultrasoft pseudopotentials [52] were used, with some exceptions[2]. In Fe, Co and Ni, non-linear core corrected pseudopotentials were used to account for the ferromagnetism. The influence of local density approach (LDA) [53] and norm-conserving pseudopotentials on the surface stress was also examined in the case of the unreconstructured (1 × 1) Pt{110} and Ir{110} surfaces.

The k-space sampling parameters, i.e. energy cut-off, E_{cut}, and Monkhorst–Pack (MP) grids [54], were chosen in bulk

[1] The expression derived in the stress theorem for the exchange and correlation contribution to the bulk stress is, within a local theory, $\tau^{\mathrm{xc}}_{ij} = \frac{1}{V}\delta_{ij}\int n(\vec{r})(\epsilon_{\mathrm{xc}}[n(\vec{r})]-\mu_{\mathrm{xc}}[n(\vec{r})])\mathrm{d}\vec{r}^3$ where $n(\vec{r})$ is the electron density, ϵ_{xc} is the exchange and correlation functional and μ_{xc} the exchange and correlation potential $\mu_{\mathrm{xc}}[n] = \frac{\delta(n\epsilon_{\mathrm{xc}})}{\delta n}$. Assuming the simple Slater form for the functional $\epsilon_{\mathrm{xc}} = -\alpha n^{1/3}$, τ^{xc} is always tensile, regardless of the external pressure P applied to the system (intuitively, τ^{xc} is tensile as it accounts for Coulomb interactions between an electron and its exchange and correlation hole). P relates to the total energy of the system, at an equilibrium volume V for that P, through a virial theorem, for example $3PV = 2T + U - 3V\tau^{\mathrm{xc}}$ [61], where T and U are the kinetic and potential energies, respectively. In the surface, we expect a lower electron density than in the bulk, and thus a compressive σ^{xc}.

[2] The ultrasoft pseudopotentials provided within the CASTEP distribution for W yield unrealistic values of the surface energy and may be in error. Norm-conserving pseudopotentials were used instead for this case.

Table 1. Calculation parameters. Monkhorst–Pack (MP) sampling corresponds to the close-packed cases, i.e. {110} in bcc, {111} in fcc and {0001} in hcp metals. Last column shows the converged bulk moduli, B. The experimental values [55] are given in parenthesis. More details on the Fe, Mo and W calculations can be found elsewhere [46].

	k-points	E_{cut} (eV)	a (Å)	c (Å)	B (GPa)
Fe	15 × 15 × 1	380	2.816		210(169)
Co	18 × 18 × 1	360	2.515	4.073	210(190)
Ni	16 × 16 × 1	380	3.540		192(186)
Mo	18 × 18 × 1	330	3.144		301(260)
Ru	20 × 20 × 1	400	2.719	4.286	309(311)
Rh	14 × 14 × 1	330	3.852		263(270)
Pd	12 × 12 × 1	360	3.906		187(193)
W	20 × 20 × 1	480	3.161		308(310)
Re	20 × 20 × 1	370	2.756	4.444	376(367)
Ir	18 × 18 × 1	370	3.858		387(355)
Pt (PW91)	16 × 16 × 1	320	3.973		256(283)
Pt (LDA)	16 × 16 × 1	300	3.922		314(283)

calculations for each species under study, where the lattice constants were optimized within a 0.002 Å error bar, and with tolerances of 2 meV per atom in total energies and 0.01 GPa in the cell stress and 4 GPa in the bulk moduli. Thus obtained convergence parameters are summarized in table 1. Slab calculations were carried out using these lattice constants to constrain the lateral periodicity. Slabs contained 14 atomic layers and were separated by the equivalent of ten atomic layers of vacuum. The three outer atomic layers were allowed to relax at each side of the slab.

Stress on the supercell is calculated by CASTEP by extension of the Hellmann–Feynman theorem [27]. The result is a three-dimensional tensor. In slab calculations, the surface contribution is extracted by applying [29]:

$$\sigma_{ij} = \frac{c}{2}\left(\tau_{ij}^{(\text{slab})} - \frac{N^{(\text{slab})}}{N^{(\text{bulk})}}\tau_{ij}^{(\text{bulk})}\right) \tag{1}$$

where c is the supercell height, $N^{(\text{slab})}$ is the number of atoms in the slab, and $[\tau_{ij}^{(\text{slab})}]$ is the (three-dimensional) supercell stress. $N^{(\text{bulk})}$ and $[\tau_{ij}^{(\text{bulk})}]$ correspond to the supercell number of atoms and stress, respectively, when the supercell is completely filled in with atomic planes (equivalent to a bulk calculation). This equation correlates with the idea of $[\sigma_{ij}]$ being an *excess quantity* with respect to the stress in the bulk [12]. The expression above is thus independent of the state of strain in the slab. In practice, even in equilibrium, the bulk calculation yields a spurious numerical contribution that is removed when using equation (1).

Stress in a crystal arises as a balanced competition between kinetic repulsive terms (negative, compressive), and attractive (positive, tensile) terms of electrostatic nature. Exchange and correlation also provide a small tensile contribution. The surface stress can be split into these components, according to the interpretation made in [30]:

$$\sigma_{ij} = \sigma_{ij}^{\text{kin}} + \sigma_{ij}^{\text{ele}} + \sigma_{ij}^{\text{xc}}. \tag{2}$$

In the context of the present work, where stresses are evaluated using the stress theorem, this splitting is meaningful. This would not be true if the surface stresses had been calculated according to the electrostatic forces method [22]. Each of the terms in equation (2) is itself an excess quantity of the type of equation (1), that allows comparison between different systems. Three-dimensional stress components depend on calculation parameters, such as the pseudopotentials and functional. The contribution of the surface is thus isolated and well defined, regardless of the calculation details [30, 42] (the influence of different functional and pseudopotential choices will be examined for Pt, though). The terms corresponding to the wavefunction derivatives in the Hellmann–Feynman theorem are not included in that interpretation (terms that cancel each other in the ground state when the stress components are added up), i.e. the components above do not have a one-to-one corresponding energy term [30, 42, 31]. By comparison to the jellium model [41], it has been predicted that $[\sigma_{ij}^{\text{kin}}] < 0$, $[\sigma_{ij}^{\text{ele}}] > 0$ and $[\sigma_{ij}^{\text{xc}}] < 0$ [30, 42] (see footnote 1).

Table 2. Calculated relaxed interlayer spacing with respect to the bulk spacing for selected hcp{0001} and fcc{111} surfaces.

	Δ_1 (%)	Δ_2 (%)	Δ_3 (%)
Co	−2.55	1.34	−0.48
Ni	−1.02	−0.25	0.59
Ru	−3.80	0.20	0.44
Rh	−2.02	−1.55	−0.29
Pd	0.55	−0.06	0.25
Re	−6.03	3.43	−1.75
Ir	−1.91	−0.47	0.22
Pt (PW91)	1.37	0.32	0.58
Pt (LDA)	0.77	−0.23	−0.13

The surfaces examined in this work have been chosen such that they provide information about the stress behaviour as a function of the structure, via the close packing and the bulk crystal symmetry, and of the atomic species, covering different cases of d-band filling and d period. The elements under study are bcc Fe, Mo and W; hcp Co, Ru and Re; and fcc Rh, Ir, Ni, Pd and Pt. The surfaces considered to account for close packing are bcc{110}, fcc{111} and hcp{0001}, and for close packing in one dimension, bcc{211}, fcc{110} and hcp{10$\bar{1}$0}.

3. Results

First, we have analysed the dependence of the surface stress as a function of the functional form and the pseudopotential details for Pt{111} and Pt{110}, using both ultrasoft pseudopotentials and norm-conserving pseudopotentials, and both LDA and GGA-PW91 functionals. The obtained relaxed geometries are summarized in tables 2 and 3, and the stress components are in tables 4 and 5. The stress on the unrelaxed Pt{110} surfaces and other values in the literature are shown in table 6.

At Pt{111}, our LDA σ values are in good agreement with $\sigma = 0.392$ and $0.350\,\text{eV Å}^{-2}$ found in LDA-based calculations in [31] and [56], respectively. They are also in reasonable agreement with the ones made by Feibelman [28] and Olivier *et al* [20] within the LDA, although ours are slightly smaller. There are also some discrepancies in the relaxed geometries with respect to [28].

Table 3. Relaxed interlayer spacing with respect to bulk in fcc{110} and hcp{10$\bar{1}$0} surfaces. Other values from the literature are shown for a comparison.

	Δ_1 (%)	Δ_2 (%)	Δ_3 (%)
Co	−7.11	1.37	−0.15
Ni	−10.89	3.72	−0.96
Ni experiment ([57])	-8.4 ± 0.8	3.1 ± 1	—
Ru	−6.61	−0.88	−0.44
Rh	−10.99	2.77	0.08
Pd	−8.11	3.27	0.77
Pd ([28], LDA)	−9.0	3.3	−0.5
Re	−8.30	−0.28	−0.22
Ir	−12.29	4.64	−1.21
Pt (PW91)	−13.81	7.38	−1.56
Pt (LDA)	−13.62	7.32	−1.63
Pt ([28], LDA)	−11.6	5.4	−1.6

Table 4. Stress components for Pt-{111} in different types of calculations. Labels PW91 and LDA refer to the functional, and 'us' and 'nc' mean ultrasoft and norm-conserving pseudopotential, respectively. Units are eV Å^{-2}.

	Total	Kinetic	XC	Electrostatic
Pt (us, PW91)	0.392	0.559	−0.082	−0.085
Pt (nc, PW91)	0.377	0.952	−0.086	−0.493
Pt (us, LDA)	0.385	0.567	−0.085	−0.094
Pt (nc, LDA)	0.396	0.983	−0.089	−0.501

Table 5. Stress components for Pt{110}-(1 × 1) in different calculations, parallel and perpendicular to the dense direction [1$\bar{1}$0]. Labels PW91 and LDA refer to the functional, and 'us' and 'nc' mean ultrasoft and norm-conserving pseudopotential, respectively. Units are eV Å^{-2}.

		Total	Kinetic	XC	Electrostatic
Pt (us, PW91)	∥	0.212	0.437	−0.061	−0.164
	⊥	0.028	0.089	−0.046	−0.15
Pt (nc, PW91)	∥	0.224	0.819	−0.063	−0.532
	⊥	0.037	0.053	−0.048	−0.031
Pt (us, LDA)	∥	0.213	0.541	−0.073	−0.615
	⊥	0.021	0.153	−0.073	−0.002
Pt (nc, LDA)	∥	0.292	0.988	−0.075	−0.621
	⊥	0.077	0.120	−0.075	0.033

3.1. Close-packed surfaces

Figure 1 shows bar plots of the decomposition of σ into components for the isotropic surfaces, including fcc{111} and hcp{0001} surfaces. The corresponding relaxed geometries appear in table 2, where contraction is the general feature, with Pt and Pd as exceptions. The anomalous expansion in Pt{111} seems to be inconsistent with the usual argument that a contraction of surface planes would relieve stress by strengthening the bonds [22]. As pointed out by Feibelman, the inconsistency appears to be solved by the fact that unfilled states in Pt are antibonding, so adding electrons there would weaken rather than strengthen the bonds [31].

In the bcc{110} surfaces, which are close-packed and anisotropic, the total stresses and the decomposition into components is shown for directions [1$\bar{1}$0] and [001] in figure 2. Further details about calculations on these structures can be found elsewhere [46]. The origin of relaxations in 4d close-packed metals has been proposed to lie in the depletion of sp electrons at the surface plane [59].

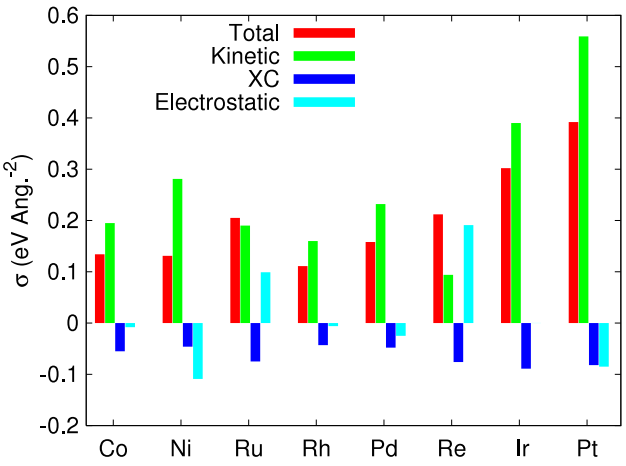

Figure 1. Bar graph of electronic stress components in isotropic surfaces, i.e. fcc{111} and hcp{0001} cases. The values for Pt{111} correspond to the usual ultrasoft pseudopotential and GGA calculation.

Table 6. Stress in one-dimensional close-packed surfaces, both unrelaxed (unr) and relaxed (rel), parallel and perpendicular to the dense direction. Results for Pt{110}-(1 × 1) with different functionals and literature values are also shown. Units are eV Å^{-2}.

	$\sigma_{\parallel}^{\mathrm{unr}}$	$\sigma_{\perp}^{\mathrm{unr}}$	$\sigma_{\parallel}^{\mathrm{rel}}$	$\sigma_{\perp}^{\mathrm{rel}}$
Fe	0.059	0.148	0.061	0.151
Ni	0.173	0.172	0.125	0.096
Ni ([58], PBE)	—	—	0.120	0.097
Ni ([20], LDA)	—	—	0.156	0.125
Mo	0.348	0.326	0.177	0.153
Ru	0.299	0.278	0.208	0.122
Rh	0.202	0.190	0.143	0.079
Rh ([20], LDA)	—	—	0.191	0.156
Pd	0.153	0.128	0.118	0.078
Pd ([20], LDA)	—	—	0.156	0.095
Pd ([28], LDA)	0.236	0.224	0.171	0.116
W	0.439	0.362	0.230	0.141
Re	0.401	0.495	0.221	0.309
Ir	0.406	0.286	0.278	0.084
Ir ([20], LDA)	—	—	0.313	0.107
Pt (PW91)	0.324	0.211	0.212	0.028
Pt (LDA)	0.407	0.276	0.278	0.066
Pt ([28], LDA)	0.453	0.309	0.317	0.113
Pt ([20], LDA)	—	—	0.308	0.099

Excluding Mo, W and Re, the total stress is mainly contributed by the kinetic term, as shown in the bar graphs. Only Mo, W, Ru and Re have a positive electrostatic component. Fe has also a very small positive electrostatic component in the [001] direction.

3.2. One-dimensional close-packed surfaces

In the bcc{211}, hcp{10$\bar{1}$0} and fcc{110} surfaces, where a close-packed chain of atoms is the main structural characteristic, a variety of anisotropy behaviours is present for different species, which is summarized in figure 3 at directions

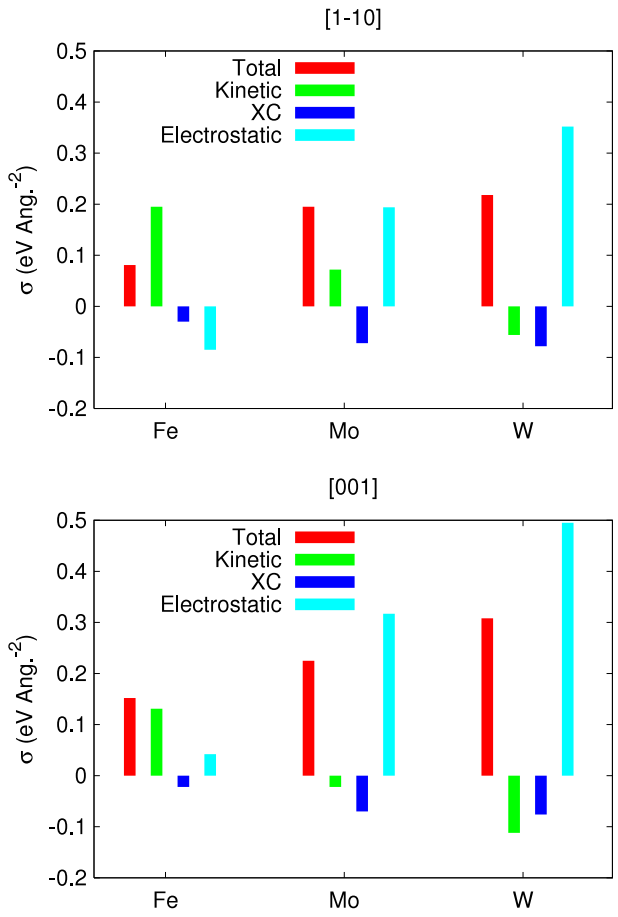

Figure 2. Bar graph of electronic stress components in (anisotropic) bcc{110} surfaces. Calculation details can be found elsewhere [46].

parallel and perpendicular to the close-pack direction, $\sigma_{\parallel}$ and $\sigma_{\perp}$, respectively. The anisotropy of those stresses, $A = \sigma_{\perp}/\sigma_{\parallel}$, is also shown there. Agreement of fcc{110} stresses with values from the literature is reasonable, as shown in table 6. It is observed there that LDA calculations tend to overestimate the stresses. Only Fe and Re show an anisotropy significantly greater than unity, i.e. major principal stress perpendicular to the dense direction. Co and Mo are rather isotropic. Table 3 contains the relaxed structure for the fcc and hcp cases, while the bcc ones can be found in [46]. The bulk-terminated stresses show that a significant stress relief occurs during relaxation at $\sigma_{\perp}$ (see table 6). The general trend is that the topmost interlayer distance, Δ_1, contracts by $\sim$10 %. In all the fcc cases, this relaxation reduces all lengths but two in the bonds supported by a surface atom (those two bonds are the in-plane ones along the dense direction $[1\bar{1}0]$), causing a large tensile $\sigma_{\perp}$ relief. It can be argued that $\sigma_{\parallel}$ is less reduced because of the constrained bonds along $[1\bar{1}0]$. In Ru and Re, relief is smaller, but we cannot attribute the unusual anisotropy in Re to relaxations, since also the unrelaxed surface shows $A > 1$. The Fe{211} case is more extreme, as relaxation relieves no stress.

4. Discussion

In Pt{111}, as shown in table 4, the total stress value is not affected by the PW91 or LDA functional choice (the LDA value in the literature, $\sigma = 0.35$ eV Å^{-2} [60], is in agreement), and even the individual components are similar for PW91 and LDA. In Pt{110}, LDA overestimates $[\sigma_{ij}]$, especially along $[1\bar{1}0]$. However, this discrepancy is not only contributed by differences in σ^{xc}, but also by a larger σ^{kin} in the LDA case.

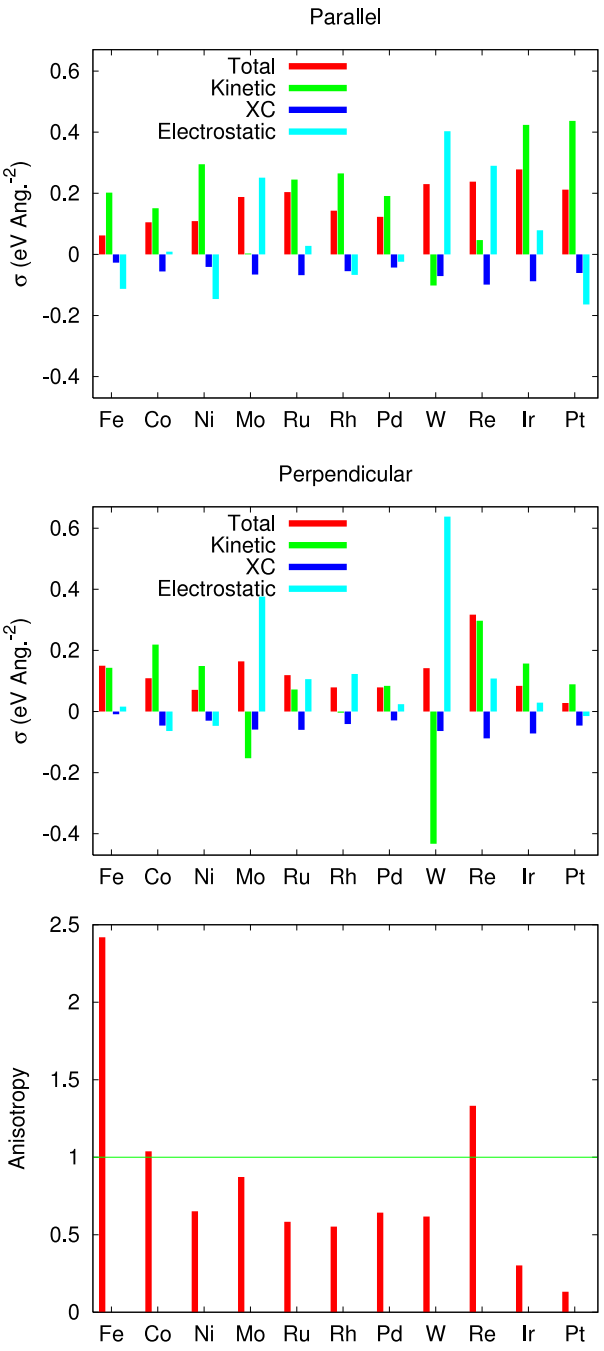

Figure 3. Bar graph of electronic stress components in one-dimensional close-packed surfaces fcc{110}, hcp{10$\bar{1}$0} and bcc{211}. The values for Pt{110} correspond to the usual ultrasoft pseudopotential and GGA calculation. The bottom panel shows the anisotropy in the total stresses calculated as $\sigma_{\perp}/\sigma_{\parallel}$.

In principle, the pseudopotential choice should not alter the surface stress, as long as it provides an accurate ground state (calculations made for Pt with both pseudopotentials include relativistic effects, as they are key to reproduce a

lower γ in the missing row reconstruction [20]). This is verified for both Pt{111} and Pt{110} PW91 calculations. The electronic components are different though, and the difference is also strongly anisotropic. In Pt{111}, σ^{kin} nearly doubles its magnitude if norm-conserving pseudopotentials are used, and σ^{ele} is modified accordingly. However, in Pt{110}, this happens only along $[1\bar{1}0]$, while the perpendicular components are little affected by the pseudopotential nature. This pseudopotential effect persists also in LDA calculations. The norm conservation constraint implies that a different amount of valence charge is being considered, leading to larger kinetic and electrostatic components.

The fact that LDA cannot yield an anisotropic σ^{xc} is not critical for the total stress, and partial agreement between PW91 and LDA stresses exists, albeit LDA magnitudes are larger (table 4). LDA gives a smaller a_0, as expected, but this does not relieve tensile stress on the surface with respect to the PW91 prediction.

Next, we give some qualitative arguments to explain the σ^{kin} and σ^{ele} signs. Since d orbitals are directional and to some extent charge is localized, we can speak in terms of 'dangling bonds' at the surface created at the time of the solid cleavage. In surfaces of metals with filling d^n, $n < 5$, the charge that partially occupied the dangling bonds can be relocated into the surface region bonds, which are partially occupied as well. This charge relocation (the electron density increases in the surface) is consistent with the kinetic term becoming more compressive and the electrostatic more tensile when a surface is present in the crystal. And conversely, when $n > 5$, the charge at the dangling bonds at the time of cleavage cannot be relocated in the surface bonds because they are already full. In this case, part of the charge in the surface bonds is transferred to the dangling bonds, so there is electron charge density spilling in the vacuum. Thus the charge density in the surface becomes smaller, and this is consistent with the kinetic term becoming less compressive and the electrostatic less tensile when a surface exists in the crystal. In all the examined cases, as expected for a metallic surface, the sum of kinetic and electrostatic surface stress components yield a total positive tensile surface stress overall. Therefore, in early TMs stress is dominated by a tensile electrostatic component and in late TMs it is dominated by a tensile kinetic component, modified somewhat by a smaller tensile or compressive electrostatic component.

In the close-packed surfaces, the argument above is held for the late d metals Ni, Pd and Pt{111}, as clearly shown in figure 1, where $\sigma^{\text{kin}} > 0$ and it is large in magnitude, while $\sigma^{\text{ele}} < 0$. The same happens in Co, Rh and Ir{111}, but σ^{ele} is smaller in magnitude. Re and Ru{0001}, in the centre of the periodic table, have both $\sigma^{\text{kin}} > 0$ and $\sigma^{\text{ele}} > 0$ (figure 1). The corresponding results for anisotropic close-packed bcc{110} surfaces are shown in figure 2. In the early d metals Mo and W{110}, the behaviour is opposite to that of Ni, Pd and Pt{111}, i.e. $\sigma^{\text{kin}} < 0$ and small, and $\sigma^{\text{ele}} > 0$ and dominating the total stress in the two inequivalent crystallographic directions $[1\bar{1}1]$ and $[\bar{1}11]$ (in the case of W the magnitude of $\sigma^{\text{ele}} > 0$ may be amplified by the fact that a norm-conserving pseudopotential was used). Fe{110} behaviour is consistent with later d metals, although the sign of σ^{ele} varies azimuthally.

The surface energy has a characteristic volcano shape across the d band, and increases in magnitude as we move from 3d to 5d metals [47]. A simple model of square d-band monotonic filling suffices to explain qualitatively this behaviour, with the exception of magnetic 3d metal surfaces [49]. Surface termination does not influence the basics of that result. The stresses found in the present work have, however, a less predictable behaviour. It has been proposed for 4d metals, though, that a parabolic trend exists also for the stress [59], but the intermediate elements stresses present oscillations in their values.

In general, we observe that the stress increases in magnitude in 5d metals, compared with 3d and 4d metals, and also that it tends to be larger in late TMs in the isotropic cases (figure 1). Anisotropy is relevant even in close-packed surfaces, e.g. Fe{110} has a ratio $\sigma_{[1\bar{1}0]}/\sigma_{[001]} \sim 0.5$ while Mo and W{110} are less anisotropic.

The anisotropic cases of fcc{110}, hcp$\{10\bar{1}0\}$ and bcc{211}, shown in figure 3, allow packing and anisotropy effects to be added to the analysis. The sign distribution along the close-packed direction is the same as in the flat close-packed surfaces discussed above, i.e. the stress is due mainly to kinetic (electrostatic) effects in late (early) TM surfaces. However, the magnitudes along that direction do not increase downwards and to the right-hand side in the periodic table, but oscillate around $\sim$0.2 eV Å^{-2}. We cannot extract any general trend, neither for the behaviour of total stress and its components perpendicular to the dense direction, nor even for the signs. Anisotropy in Rh, Pd, Ir and Pt is strong, with the total stress being elongated parallel to the dense direction, and in Fe{211} the behaviour is inverted. We can rule out differences between the bcc{211} and fcc{110} structures as the underlying reason, since Mo and W also disagree with Fe [46]. In fact, the anisotropy of $[\sigma_{ij}^{\text{kin}}]$ and $[\sigma_{ij}^{\text{ele}}]$ components in Fe is in agreement with that of late TMs, i.e. larger along the dense direction, but they amount overall to an inverted $[\sigma_{ij}]$. In the other studied metals, anisotropy is less pronounced.

Unlike in the bcc{211} case, in the three bcc{110} surfaces, $[\sigma_{ij}]$ anisotropy is the same [46], and so it is for the main components, with $[\sigma_{ij}^{\text{kin}}]$ being the dominating term in Fe, and $[\sigma_{ij}^{\text{ele}}]$ in both Mo and W (see figure 2). As noted previously, the intrinsically chiral bcc{321} surface, consisting of a combination of {110} and {211} facets, shows an asymmetrically rotated stress tensor. Its orientation results from the interpolative combination of the stresses on the facets [46]. Thus, the electronic structure of surface bonds dictates the basic features of surface stress magnitude and anisotropy at low-index facets. When extra complex structural features are present, like facet combination in high-index surfaces, surface stress follows (at least qualitatively) an interpolative behaviour.

The above discussion can be made regardless of surface relaxations. Bond contraction or elongation by surface relaxation rearranges the charge density, and should thus correlate with the stress value, although it does not affect the anisotropy trends in the stress.

Ferromagnetism in Fe can be ruled out as the reason for Fe{211} exceptional anisotropy. Calculations imposing spin pairing have been carried out on fcc Fe{110} within the LDA. The nearest neighbour distance in non-magnetic fcc Fe is $d_0 = 2.377$ Å, and relaxations follow a similar trend to those found in one-dimensional close-packed surfaces (see table 3): about -15%, $+5\%$ and -1% in the outer interlayer spacings. The resulting surface stresses, $\sigma_{\parallel} = 0.183$ eV Å^{-2} and $\sigma_{\perp} = 0.216$ eV Å^{-2}, result in an anisotropy factor $A = 1.18$, smaller than that of ferromagnetic Fe{211} but yet inverted with respect to other metals. The use of GGA for the exchange and correlation does not alter this result, but yields smaller stress values $\sigma_{\parallel} = 0.137$ eV Å^{-2} and $\sigma_{\perp} = 0.157$ eV Å^{-2}, larger $d_0 = 2.429$ Å and comparable atomic relaxations.

5. Conclusions

The surface stress in representative d-band metal low Miller index surfaces has been calculated by means of DFT and analysed in terms of its electronic structure components: electrostatic (attractive), kinetic (repulsive) and exchange and correlation. The results for close-packed surfaces show that in early d-band metals stress has predominantly an electrostatic origin, while it has a mainly kinetic character in late d-band metals. This can be accounted for by a simple model of charge relocation if we assume that directionality of bonds in d-band metals creates dangling bonds upon surface cleavage: in early d-band species, charge from the dangling bonds is relocated into the surface bonds to strengthen them, whereas in late d-band species, charge is removed from the surface bonds to fill in the unoccupied dangling bonds.

Anisotropic surfaces containing one in-plane close-packed chain of atoms have also been studied. In these cases, the surface stress major principal axis lies parallel to the close-packed direction, being the late d metals the most anisotropic. Fe and Re are exceptions, and Fe in particular shows a strong 'inverse' anisotropy. The corresponding unrelaxed surfaces also show this behaviour. Therefore, it cannot be associated with stress relief along a particular crystallographic direction due to atomic relaxation. This behaviour must have its origin in the nature of the atomic species, rather than in the crystal structure. Ferromagnetism in Fe is also disconnected from this anisotropic effect.

Acknowledgments

MBR acknowledges financial support from the European Commission through a Marie Curie Intra-European Fellowship. SJJ acknowledges The Royal Society (UK) for a University Research Fellowship.

References

[1] Shuttleworth R 1950 *Proc. Phys. Soc.* A **63** 444
[2] Kramer D and Weissmüller J 2007 *Surf. Sci.* **601** 3042
[3] Marichev V A 2008 *Surf. Sci.* **602** 1131
[4] Kramer D and Weissmüller J 2008 *Surf. Sci.* **602** 1133
[5] Bottomley D J, Makkonen L and Kolari K 2009 *Surf. Sci.* **603** 97
[6] Marichev V A 2009 *Surf. Sci.* **603** 2345
[7] Bottomley D J, Makkonen L and Kolari K 2009 *Surf. Sci.* **603** 2347
[8] Eriksson J C and Rusanov A I 2009 *Surf. Sci.* **603** 2348
[9] Bottomley D J, Makkonen L and Kolari K 2009 *Surf. Sci.* **603** 2350
[10] Ibach H 2009 *Surf. Sci.* **603** 2352
[11] Bottomley D J, Makkonen L and Kolari K 2009 *Surf. Sci.* **603** 2356
[12] Müller P and Saúl A 2004 *Surf. Sci. Rep.* **54** 157
[13] Wolf D 1993 *Phys. Rev. Lett.* **70** 627
[14] Needs R J 1993 *Phys. Rev. Lett.* **71** 460
[15] Chou M Y, Wei S and Vanderbilt D 1993 *Phys. Rev. Lett.* **71** 461
[16] Wolf D 1993 *Phys. Rev. Lett.* **71** 462
[17] Filippetti A and Fiorentini V 1999 *Phys. Rev.* B **60** 14366
[18] Lazzeri M and Selloni A 2001 *Phys. Rev. Lett.* **87** 266105
[19] Olivier S, Tréglia G and Sául A 2003 *Surf. Sci.* **212** 866
[20] Olivier S, Tréglia G, Sául A and Willaime F 2006 *Surf. Sci.* **600** 5131
[21] Müller P and Kern R 1994 *Surf. Sci.* **301** 386
[22] Ibach H 1997 *Surf. Sci. Rep.* **29** 193
[23] Nielsen O H and Martin R M 1983 *Phys. Rev. Lett.* **50** 697
[24] Nielsen O H and Martin R M 1985 *Phys. Rev.* B **32** 3780
[25] Nielsen O H and Martin R M 1985 *Phys. Rev.* B **32** 3792
[26] Vanderbilt D 1987 *Phys. Rev. Lett.* **59** 1456
[27] Payne M C, Teter M P, Allan D C, Arias T A and Joannopoulos J D 1992 *Rev. Mod. Phys.* **64** 1045
[28] Feibelman P J 1995 *Phys. Rev.* B **51** 17867
[29] Needs R J 1987 *Phys. Rev. Lett.* **58** 53
[30] Needs R J and Godfrey M J 1987 *Phys. Scr.* **T19** 391
[31] Feibelman P J 1997 *Phys. Rev.* B **56** 2175
[32] Müller J E, Dahmen K and Ibach H 2002 *Phys. Rev.* B **66** 235407
[33] Haiss W 2001 *Rep. Prog. Phys.* **64** 591
[34] Pan W, Popescu R, Meyerheim H L, Sander D, Robach O, Ferrer S, Lin M-T and Kirschner J 2005 *Phys. Rev.* B **71** 174439
[35] Harrison M J, Woodruff D P and Robinson J 2005 *Phys. Rev.* B **72** 113408
[36] Hong S, Kara A, Rahman T S, Heid R and Bohnen K P 2004 *Phys. Rev.* B **69** 195403
[37] Harrison M J, Woodruff D P, Robinson J, Sander D, Pan W and Kirschner J 2006 *Phys. Rev.* B **74** 165402
[38] Sander D, Linke U and Ibach H 1992 *Surf. Sci.* **272** 318
[39] Harrison M J, Woodruff D P and Robinson J 2008 *Surf. Sci.* **602** 226
[40] Sander D, Enders A and Kirschner J 1999 *Europhys. Lett.* **45** 208
[41] Lang N D and Kohn W 1970 *Phys. Rev.* B **1** 4555
[42] Needs R J and Godfrey M J 1990 *Phys. Rev.* B **42** 10933
[43] Mansfield M and Needs R J 1991 *Phys. Rev.* B **43** 8829
[44] Kiejna A and Ziesche P 1993 *Solid State Commun.* **88** 143
[45] Annett J F and Inglesfield J E 1989 *J. Phys.: Condens. Matter* **1** 3645
[46] Blanco-Rey M, Pratt S J and Jenkins S J 2009 *Phys. Rev. Lett.* **102** 026102
[47] Skriver H L and Rosengaard N M 1992 *Phys. Rev.* B **46** 7157
[48] Vitos L, Ruban A V, Skriver H L and Kollár J 1998 *Surf. Sci.* **411** 186
[49] Aldén M, Skriver H L, Mirbt S and Johansson B 1992 *Phys. Rev. Lett.* **69** 2296
[50] Clark S J, Segall M D, Pickard C J, Hasnip P J, Probert M J, Refson K and Payne M C 2005 *Zeit. Krystallogr.* **220** 567
[51] Perdew J P and Wang Y 1992 *Phys. Rev.* B **45** 13244
[52] Vanderbilt D 1990 *Phys. Rev.* B **41** 7892
[53] Ceperley D M and Alder B J 1980 *Phys. Rev. Lett.* **45** 566

[54] Monkhorst H J and Pack J D 1976 *Phys. Rev.* B **13** 5188
[55] Lide D R (ed) 2009 *CRC Handbook of Chemistry and Physics* 90th edn (Boca Raton, FL: CRC Press)
[56] Needs R J, Godfrey M J and Mansfield M 1991 *Surf. Sci.* **242** 215
[57] Gauthier Y, Baudoing R, Jolyt Y, Gaubertt C and Rundgren J 1984 *J. Phys. C: Solid State Phys.* **17** 4547
[58] Harrison M J, Woodruff D P and Robinson J 2004 *Surf. Sci.* **572** 309
[59] Kádas K, Nabi Z, Kwon S K, Vitos L, Ahuja R, Johansson B and Kollár J 2006 *Surf. Sci.* **600** 395
[60] Needs R J and Mansfield M 1989 *J. Phys.: Condens. Matter* **1** 7555
[61] Janak J F 1974 *Phys. Rev.* B **9** 3985